

1 **Effect of sporadic destratification, seasonal overturn and**
2 **artificial mixing on CH₄ emissions from a subtropical**
3 **hydroelectric reservoir**

4 **F. Guérin^{1,2,3,*}, C. Deshmukh^{1,4,5,a}, D. Labat¹, S. Pighini^{6,b}, A Vongkhamsao⁶, P.**
5 **Guédant⁶, W. Rode⁶, A. Godon^{6,c}, V. Chanudet⁷, S. Descloux⁷, D. Serça⁴**

6 [1]{Université de Toulouse ; UPS GET, 14 Avenue E. Belin, F-31400 Toulouse, France}

7 [2]{IRD ; UR 234, GET ; 14 Avenue E. Belin, F-31400, Toulouse, France}

8 [3]{Departamento de Geoquímica, Universidade Federal Fluminense, Niteroi-RJ, Brasil}

9 [4]{Laboratoire d'Aérodologie - Université de Toulouse - CNRS UMR 5560; 14 Av. Edouard
10 Belin, F-31400, Toulouse, France}

11 [5]{Centre for Regulatory and Policy Research, TERI University, New Delhi, India}

12 [6]{Nam Theun 2 Power Company Limited (NTPC), Environment & Social Division – Water
13 Quality and Biodiversity Dept.– Gnommalath Office, PO Box 5862, Vientiane, Lao PDR}

14 [7]{Electricité de France, Hydro Engineering Centre, Sustainable Development Dpt, Savoie
15 Technolac, F-73373 Le Bourget du Lac, France}

16 [a]{now at: Nam Theun 2 Power Company Limited (NTPC), Environment & Social Division
17 – Water Quality and Biodiversity Dept.– Gnommalath Office, PO Box 5862, Vientiane, Lao
18 PDR}

19 [b]{now at: Innsbruck University, Institute of Ecology, 15 Sternwartestrasse, A-6020
20 Innsbruck, Austria and Foundation Edmund Mach, FOXLAB-FEM, Via E. Mach 1, IT-38010
21 San Michele all'Adige, Italy}

22 [c]{now at: Arnaud Godon Company, 44 Route de Genas, Nomade Lyon, 69003 Lyon,
23 France}

24

25 *Correspondence to: F Guérin (Frederic.guerin@ird.fr)

26 **Abstract**

27 Inland waters in general and specifically freshwater reservoirs are recognized as source of
28 CH₄ to the atmosphere. Although the diffusion at the air-water interface is the most studied
29 pathway, its spatial and temporal variations are poorly documented.

30 We measured fortnightly temperature and O₂ and CH₄ concentrations parameters at nine
31 stations in a subtropical monomictic reservoir which was flooded in 2008 (Nam Theun 2
32 Reservoir, Lao PDR). Based on these results, we quantified CH₄ storage in the water column
33 and diffusive fluxes from June 2009 to December 2012. We compared diffusive emissions
34 with ebullition from Deshmukh et al. (2014) and aerobic methane oxidation and downstream
35 emissions from (Deshmukh et al., 2016).

36 In this monomictic reservoir, the seasonal variations of CH₄ concentration and storage were
37 highly dependant of the thermal stratification. Hypolimnic CH₄ concentration and CH₄
38 storage reached their maximum in the warm dry season (WD) when the reservoir was
39 stratified. They decreased during the warm wet (WW) season and reached its minimum after
40 the reservoir overturned in the cool dry season (CD). The sharp decreases of the CH₄ storage
41 were concomitant with sporadic extreme diffusive fluxes (up to 200 mmol m⁻² d⁻¹). These hot
42 moments of emissions occurred mostly in the inflow region in the WW season and during the
43 overturn in the CD season in the area of the reservoir that has the highest CH₄ storage.
44 Although they corresponded to less than 10% of the observations, these CH₄ extreme
45 emissions (>5 mmol m⁻² d⁻¹) contributed up to 50% of total annual emissions by diffusion.

46 During the transition between the WD and WW seasons, a new hotspot of emissions was
47 identified upstream of the water intake where diffusive fluxes peaked at 600 mmol m⁻² d⁻¹ in
48 2010 down to 200 mmol m⁻² d⁻¹ in 2012. In the CD season, diffusive fluxes from this area
49 were the lowest observed at the reservoir surface. Emissions from this area contributed 15-
50 25% to total annual emissions although they occur on a surface area representative of less
51 than 1% of the total reservoir surface. We highly recommend measurements of diffusive
52 fluxes around water intakes in order to evaluate if such results can be generalized.

53 **1. Introduction**

54 Since the 1990s, hydroelectric reservoirs are known to be source of methane (CH₄) to the
55 atmosphere. Their contribution to total CH₄ emissions still needs refinement since the
56 discrepancies among estimates is large, ranging from 1 to 12% of total CH₄ emissions (St
57 Louis et al., 2000;Barros et al., 2011). These two estimates are mostly based on diffusive

58 fluxes at the air-water interface and they overlook emissions from the rivers downstream of
59 the dams (Abril et al., 2005;Guerin et al., 2006;Kemenes et al., 2007;Teodoru et al.,
60 2012;Maeck et al., 2013;Deshmukh et al., 2016), CH₄ ebullition (DelSontro et al.,
61 2010;Deshmukh et al., 2014) and emissions from the drawdown area of reservoirs (Chen et
62 al., 2009;Chen et al., 2011) although these pathways could largely dominate diffusion at the
63 surface of the reservoirs.

64 Even if CH₄ diffusion at the surface of reservoir is the best-documented emission pathway,
65 little information is available on spatial and temporal variability of CH₄ emissions by
66 diffusive fluxes. In tropical amictic reservoirs, the highest diffusive fluxes are usually
67 observed during dry periods and when the stratification weaken at the beginning of the rainy
68 season (Guerin and Abril, 2007). A study of CH₄ emissions from a dimictic reservoir suggests
69 a potential large outgassing of CH₄ during the reservoir overturns (Utsumi et al., 1998b) as it
70 is the case in natural monomictic and dimictic lakes (Kankaala et al., 2007;López Bellido et
71 al., 2009;Schubert et al., 2010;Schubert et al., 2012;Fernández et al., 2014). Such hot
72 moments of emissions (McClain et al., 2003) could contribute 45-80% of CH₄ annual
73 emissions by diffusion (Schubert et al., 2012;Fernández et al., 2014). They are rarely taken
74 into account in carbon budgets since they can only be captured by high frequency monitoring.
75 Spatial heterogeneity of CH₄ emissions at the surface of reservoirs is also very high. It mostly
76 depends on the spatial variations of ebullition that is controlled by sedimentation (DelSontro
77 et al., 2011;Sobek et al., 2012;Maeck et al., 2013). The spatial variation of diffusion appears
78 to be low with emissions being slightly higher (1) in area where dense forest is flooded as
79 compare to the former riverbed (Abril et al., 2005), (2) at shallow sites than at deeper ones
80 (Zheng et al., 2011;Sturm et al., 2014) and (3) in inflow zones of reservoirs compare to the
81 main body (Musenze et al., 2014). However, as it was shown for CO₂ emissions from a
82 tropical hydroelectric reservoir, taking into account both spatial and temporal variability of
83 emissions significantly affect carbon budgets and emission factors (Pacheco et al., 2015).

84 In the framework of a comprehensive project aiming at quantifying greenhouse gas emissions
85 from the Nam Theun 2 Reservoir (NT2R), a recently flooded subtropical located in Lao PDR,
86 we studied (1) the spatial and temporal variability of CH₄ ebullitive fluxes (Deshmukh et al.,
87 2014) and (2) the downstream CH₄ emissions (Deshmukh et al., 2016). In the present study,
88 the objective is to quantify the CH₄ diffusive fluxes at the surface of NT2R and evaluate if
89 diffusive fluxes were improperly quantified in previously published CH₄ budget due to
90 inappropriate spatial and seasonal resolution. . The CH₄ emissions were quantified fortnightly

91 during three and a half year (May 2010 to December 2012) based on a monitoring of CH₄
92 concentrations that started in June 2009. This was performed at nine stations flooding
93 different types of ecosystems. On the basis of these results, we discuss the spatial and
94 temporal variations of the CH₄ emissions by diffusive fluxes and the significance of hotspots
95 and hot moments in the total emissions from the surface of the reservoir.

96 **2. Material and methods**

97 **2.1. Study area**

98 The NT2 hydroelectric reservoir (17° 59' 49" N, 104° 57' 08" E) was built on the Nam Theun
99 River located in the subtropical region of Lao People's Democratic Republic (Lao PDR) on
100 the Nakai Plateau. A detailed description of the study site is given in Descloux et al. (2014).
101 The filling of the reservoir began in April 2008, the full water level was first reached in
102 October 2009 and the power plant was commissioned in April 2010. Annually, the NT2
103 Reservoir receives around 7527 Mm³ of water from the Nam Theun watershed, which is more
104 than twice the volume of the reservoir (3908 Mm³). A continuous flow of 2 m³ s⁻¹ (and
105 occasionally spillway release) is discharged from the Nakai Dam (ND in Fig 1) to the Nam
106 Theun River. The water used for electricity production is delivered from water intake (WI in
107 Fig 1) to the powerhouse (PH in Fig 1). The powerhouse is located in the valley 200 m below
108 the plateau.

109 Typical meteorological years are characterized by three seasons: warm wet (WW) (mid June-
110 mid October), cool dry (CD) (mid October-mid February) and warm dry (WD) (mid
111 February-mid June). Daily air temperature varies between 14°C (CD season) to 30°C (WD
112 season). The mean annual rainfall is about 2400 mm and occurs mainly (80%) in the WW
113 season.

114 During the filling of the reservoir, 489 km² of soils and different types of vegetation
115 (Descloux et al., 2011) were flooded by the end of October 2008. The water level in the
116 reservoir was nearly constant from October 2008 to April 2010. After the commissioning,
117 during the studied period (June 2009 to December 2012) the reservoir surface varied
118 seasonally and reached its maxima (489 km²) and minima (168 to 176 km² depending on the
119 years) during the WW and WD seasons, respectively. According to these water level
120 variations, the average depth is 8 m for a maximum depth of 39 m.

121 **2.2. Sampling strategy**

122 A total of nine stations (RES1-9, Figure 1) located in the reservoir were monitored fortnightly
123 in order to determine the vertical profiles of temperature and O₂ and CH₄ concentration in the
124 water column. The characteristics of the stations are given in the Table 1. Basically, three
125 stations are located on the thalweg of the former Nam Theun River (RES2, RES4, RES6)
126 whereas four other stations are located in a small embayment in the flooded dense forest
127 (RES3), flooded degraded forest (RES5), flooded swamp area (RES7) and flooded
128 agricultural land (RES8). The RES1 station is located 100 m upstream of the Nakai Dam, and
129 RES9 station is located ~1 km upstream of the water intake delivering the water to the
130 powerhouse. All samples and in situ measurements were taken in the morning or early
131 afternoon from an anchored boat. Most of the time, the boat was attached to a buoy at the
132 sampling station. When no buoy was present, an anchor was used with care in order not to re-
133 suspend surface sediments. As the sampling started from the surface, the bottom water was
134 sampled almost an hour later and should not be influenced by the perturbation generated by
135 the anchor.

136 **2.3. Experimental methods**

137 **2.3.1. Vertical profiles of oxygen and temperature**

138 Vertical profiles of O₂ and temperature were measured in situ at all sampling stations with a
139 multi-parameter probe Quanta[®] (Hydrolab, Austin, Texas) since January 2009. In the
140 reservoir, the vertical resolution was 0.5 m above the oxic–anoxic limit and 1 to 5 m in the
141 hypolimnion.

142 **2.3.2. Methane concentration in water**

143 The evolution of CH₄ concentrations has been monitored from May 2009 to December 2012
144 on a fortnightly basis. Surface samples were taken with a surface water sampler (Abril et al.,
145 2007) and other samples from the water column were taken with an Uwitec water sampler.
146 (Abril et al., 2007). Water samples were stored in serum glass vials, capped with butyl
147 stoppers, sealed with aluminium crimps and preserved with HgCl₂ (Guerin and Abril, 2007).
148 Samples were analysed within 15 days. Before gas chromatography analysis for CH₄
149 concentration, a N₂ headspace was created and the vials were vigorously shaken to ensure an

150 equilibration between the liquid and gas phases. The concentration in the water was calculated
151 using the solubility coefficient of Yamamoto et al. (1976).

152 **2.3.3. Gas chromatography**

153 Analysis of CH₄ concentrations were performed by gas chromatography (SRI 8610C gas
154 chromatograph, Torrance, CA, USA) equipped with a flame ionization detector. A subsample
155 of 0.5 ml from the headspace of water sample vials was injected. Commercial gas standards
156 (10, 100 and 1010 ppmv, Air Liquid "crystal" standards) were injected after analysis of every
157 10 samples for calibration. Duplicate injection of samples showed reproducibility better than
158 5%.

159 **2.4. Water column CH₄ storage**

160 Between two sampling depth of the vertical profiles of CH₄ concentrations, the CH₄
161 concentrations were assumed to change linearly in order to calculate the concentration in each
162 1-m layer of water. The volume of water in each layer was calculated using the volume-
163 capacity curve (NTPC, 2005). The CH₄ storage was calculated by multiplying the average
164 CH₄ concentrations of each layer by the volume of the layer and summing-up the amount of
165 CH₄ for all depth intervals.

166 **2.5. Aerobic CH₄ oxidation**

167 The depth-integrated CH₄ oxidation rates at each station were calculated on the basis of the
168 specific oxidation rates (d⁻¹) determined at NT2 (Deshmukh et al., 2016) and the vertical
169 profiles of CH₄ and O₂ concentrations in the water column as already described in (Guerin
170 and Abril, 2007). The depth-integrated CH₄ oxidation rates at each station were estimated
171 only from January 2010 since the vertical resolution of the vertical profiles of O₂ and CH₄
172 was not high enough in 2009.

173 As the aerobic methane oxidation rates we obtained were potential, CH_{4-ox} were corrected for
174 two limiting factors, the oxygen availability and the light inhibition as described in Guerin
175 and Abril (2007). The final equation to compute in situ oxidation rates (CH_{4-ox}, mmol m⁻² d⁻¹)
176 is:

$$177 \text{CH}_{4\text{-ox}} = C_{\text{CH}_4} \cdot S_{\text{CH}_4\text{-ox}} \cdot C_{\text{O}_2} / (C_{\text{O}_2} + K_m(\text{O}_2)) \cdot d \cdot I(z)$$

178 with C_{CH_4} , the CH_4 concentration; S_{CH_4-ox} , the specific CH_4-ox from Deshmukh et al. (2016);
179 C_{O_2} , the oxygen concentration; $K_{m(O_2)}$, the K_m of O_2 for CH_4 oxidation, d , depth of the water
180 layer and $I(z)$, the inhibition of methanotrophic activity by light as defined by Dumestre et al.
181 (1999) at the Petit Saut Reservoir. Finally, the CH_4 oxidation rates were integrated in the oxic
182 water column, from the water surface to the limit of penetration of oxygen.

183 **2.6. Diffusive fluxes from surface concentrations**

184 The diffusive CH_4 fluxes were calculated from the fortnightly monitoring of surface
185 concentrations with the thin boundary layer (TBL) equation at all stations in the reservoir
186 (RES1-9). The CH_4 surface concentrations in water and the average CH_4 concentration in air
187 (1.9 ppmv) obtained during eddy covariance deployments (Deshmukh et al., 2014) were
188 applied in equation (1) to calculate diffusive flux:

$$189 \quad F = k_T \times \Delta C \quad (1)$$

190 where F , the diffusive flux at water-air interface; k_T , the gas transfer velocity at a given
191 temperature (T); $\Delta C = C_w - C_a$, the concentration gradient between the water (C_w) and the
192 concentration at equilibrium with the overlying atmosphere (C_a). Afterward, the k_T was
193 computed from k_{600} with the following equation:

$$194 \quad k_T = k_{600} \times (600/Sc_T)^n \quad (2)$$

195 with Sc_T , the Schmidt number of CH_4 at a given temperature (T) (Wanninkhof, 1992); n , a
196 number that is either $2/3$ for low wind speed ($< 3.7 \text{ m s}^{-1}$) or $1/2$ for higher wind speed and
197 turbulent water (Jahne et al., 1987).

198 For the determination of k_{600} at the stations RES1-8, we used both the formulations from
199 Guerin et al. (2007) which includes the cumulative effect of wind (U_{10}) and rain (R) on k_{600}
200 ($k_{600} = 1.66e^{0.26U_{10}} + 0.66R$), and the average formulation of MacIntyre et al. (2010) ($k_{600} =$
201 $2.25 U_{10} + 0.16$) whatever the buoyancy fluxes. As shown by (Deshmukh et al., 2014), the
202 average of the fluxes obtained from these two relationships compared well with fluxes
203 measured by floating chambers at the reservoir surface and no enhancement of the CH_4 fluxes
204 could have been attributed to the variations of buoyancy fluxes when the eddy covariance
205 system was deployed. Since the water current velocities were lower than 1 cm s^{-1} in most of
206 the reservoir (Chanudet et al., 2012), the effect of water current on k_{600} was not included. For
207 calculation purpose, wind speed (at 10 m height) and rainfall from two adjacent

208 meteorological stations located at Nakai Village (close to RES9 station) and at the Ban
209 Thalang Bridge (close to RES4 station, Figure 1) were used. At these stations, the average
210 k_{600} was 6.5 cm h^{-1} over the course of the year.

211 At the water intake (RES9) where the hydrology and hydrodynamics is different from the
212 other stations, it was impossible to quantify the k_{600} since the boat drifted quickly to the
213 shoreline because of water currents in the narrow channel. According to Chanudet et al.
214 (2012), water current velocity in this area of the reservoir is about 0.2 m s^{-1} . After Borges et
215 al. (2004), the contribution of such water currents in a water body with depth ranging from 9
216 to 20 m is $2.0 \pm 0.5 \text{ cm h}^{-1}$ which should be summed up with the contribution of wind and
217 rainfall from Guerin et al. (2007) and MacIntyre et al. (2010). It gives an average of 9 cm h^{-1} .
218 The k_{600} was determined in the regulating dam (Deshmukh et al., 2014) located downstream
219 of the turbine where we visually observed vortexes similar to those observed at RES9. In the
220 regulating dam, the k_{600} was 19 cm h^{-1} on average for 4 measurements (not show). In order to
221 be conservative for the estimation of emissions from the water intake, we considered a
222 constant value of k_{600} (10 cm h^{-1}) which is in the lower range of (1) the k_{600} calculated from
223 (Guerin et al., 2007), MacIntyre et al. (2010) and Borges et al. (2004), and (2) k_{600} values
224 determined in area with comparable hydrology/hydrodynamics.

225 **2.7. Total emissions by diffusive fluxes**

226 Based on physical modelling (Chanudet et al., 2012), it has been showed that the station
227 RES9 located at the water intake is representative of an area of $\sim 3 \text{ km}^2$ (i.e. 0.6% of reservoir
228 water surface), whatever the season. This 3- km^2 area was used to extrapolate specific
229 diffusive fluxes from RES9. The embayment where RES3 is located represents a surface area
230 of 5-6% of the total surface area of the reservoir whatever the season (maximum 28 km^2), to
231 which were attributed the specific diffusive fluxes from RES3. The diffusive fluxes calculated
232 for RES1, RES2, RES4, RES5, RES6, RES7 and RES8 stations were attributed to the water
233 surface area representative for each station, taking into account the seasonal variation of the
234 reservoir water surface from the surface-capacity curve (NTPC, 2005).

235 **2.8. Statistical and correlation analysis**

236 Statistical tests were performed to assess the spatial and temporal variations in the surface
237 CH_4 concentrations and diffusive fluxes at all stations in the reservoir. Normality of the
238 concentration and diffusive datasets was tested with R software (R Development Core Team,

239 2008) and the Nortest package (Gross and Ligges, 2015). The data distribution was tested
240 with the Fitdistrplus package (Delignette-Muller et al., 2015).

241 Since all tests indicated that the distribution of the data were neither normal nor lognormal,
242 Kruskal-Wallis and Mann-Whitney tests were performed with GraphPad Prism (GraphPad
243 Software, Inc., v5.04). No significant differences were found between the seasons and/or the
244 stations. These test results were attributed to the very large range of surface concentrations
245 due to the sporadic occurrence of extreme values (over 4 orders of magnitude). In order to
246 reduce this range, the log of the concentrations was used. For each station, the time series of
247 the log of the CH₄ surface concentrations were linearly interpolated and re-sampled every 15
248 days in order to compare time series with the same number of observations. The log of the
249 concentrations was used to determine the frequency distribution, the skewness of the dataset
250 (third order moment), the auto-correlation of each time series and the correlation between the
251 different stations. All analyses were performed using Matlab.

252 **3. Results**

253 **3.1. Temperature and O₂ dynamics in the reservoir**

254 During the three and half year of monitoring at the stations RES1-8, the NT2R was thermally
255 stratified with a thermocline at 4.5 ± 2.6 m depth in the WD (Feb-Jun) season as revealed by
256 the vertical profiles of temperature (Figure 2). In the WW season, the temperature vertical
257 profiles at the stations RES1-8 either showed a thermocline (RES7 and RES8 in 2010 and
258 2011, Figure 2) whereas in some occasions, the temperature decreased regularly from the
259 surface to the bottom during sporadic destratification (RES1-3, Figure 2). On average during
260 the WW season, a thermocline was located at 5.8 ± 4.8 m depth. During the CD season, the
261 reservoir overturned as already mentioned by Chanudet et al. (2012) and the temperature was
262 constant from the surface to the bottom (Figure 2) in the different years. In order to illustrate
263 the destratification, a stratification index (ΔT) which corresponds to the difference between
264 the surface and bottom water temperature was defined. During the periods of stratification in
265 the WD seasons, ΔT was up to 10°C higher than during reservoir overturn in the CD season
266 with ΔT close to zero (Figure 3a). During the WW season, the ΔT decreased gradually.

267 During the WD season at the stations RES1-8, an oxicleine was most of the time located at a
268 depth concomitant with the depth of the thermocline whereas oxygen penetrated deeper in the
269 WW season (Figure 2). During these two seasons, the epilimnion was always well oxygenated

270 with O₂ concentrations higher than 200 μmol L⁻¹. In the WD season, the hypolimnion was
271 completely anoxic whereas O₂ reached occasionally the hypolimnion during the sporadic
272 destratification events in the WW season (29±54 μmol L⁻¹, Figure 2 and 3b). During the CD
273 season (reservoir overturn), the water column was often oxygenated from the top to the
274 bottom of the reservoir (Figure 2). On average over the whole reservoir, the lowest
275 hypolimnic oxygen concentration was observed in 2010 before the reservoir was
276 commissioned (Figure 3b).

277 After the commissioning of the reservoir (April 2010), the water column located near the
278 water intake (RES9) got totally mixed as revealed by the homogeneous temperature and
279 oxygen profiles from the surface to the bottom whatever the season (Figure 2). The water
280 column at RES9 was always well oxygenated (163 ± 62 μmol L⁻¹, Figure 2).

281 **3.2. Seasonal dynamics of the CH₄ concentration in the reservoir**

282 At the station RES1-8, when the water column is thermally stratified with a steep oxicleine in
283 the WD and often in the WW seasons, CH₄ concentrations are in average ~150 times higher in
284 the reservoir hypolimnion (246 ± 234 μmol L⁻¹) than in the epilimnion (1.6 ± 7.7 μmol L⁻¹)
285 (Figure 2). The gradient of CH₄ concentration at the thermocline/oxicleine was steeper during
286 the WD season than during the WW season (Figure 2). During the CD season, the average
287 CH₄ concentration in the reservoir bottom water lowered by a factor of three compare to the
288 WD and the WW seasons. However, the reservoir overturn increased the average CH₄
289 concentrations in the epilimnion by a factor of two (3.4 ± 14.8 μmol L⁻¹) in comparison with
290 the WD and WW seasons. After the commissioning, the CH₄ vertical profiles of concentration
291 before turbine intake (RES9) were homogeneous from the surface to the bottom. The average
292 CH₄ concentration from the surface to the bottom peaked up to 215 μmol L⁻¹ with averages of
293 39.8 ± 48.8, 29.9 ± 55.4 and 1.9 ± 4.3 μmol L⁻¹ during the WD, WW and CD seasons,
294 respectively (Figure 2). The concentrations at RES9 were up to 10 times lower than the
295 maximum bottom concentrations at the other stations for a given season. Since the station
296 RES9 behaved differently from the other stations, results from this station will be treated
297 separately.

298 The overall bottom CH₄ concentration (Figure 3c) and dissolved CH₄ stock in the reservoir
299 (Figure 3d) increased at the beginning of the WD season. The higher bottom CH₄
300 concentration and storage in the reservoir are concomitant with both the establishment of

301 anoxia in the hypolimnion and the reservoir thermal stratification (Figure 3). Hypolimnic CH₄
302 concentration and storage reached their maxima (up to $508 \pm 254 \mu\text{mol L}^{-1}$ and 4.7 ± 0.5
303 Gg(CH₄), Figure 3c,d) at the end of the WD-beginning of the WW season when the residence
304 time of water in the reservoir was the lowest (40 days, Figure 3d). Along the WW season, the
305 thermal stratification weakened (Figure 3a) and the CH₄ concentration and dissolved CH₄
306 stock decreased (Figure 3c,d) while the residence time of water increased (Figure 3d). In the
307 CD season, the reservoir overturns as evidenced by the low ΔT and the penetration of O₂ to
308 the hypolimnion (Figure 3a,b). During CD season, the bottom CH₄ concentration and the
309 storage reached their minima (down to $1.3 \pm 4.5 \mu\text{mol L}^{-1}$ and $0.01 \pm 0.001 \text{ Gg(CH}_4\text{)}$, Figure
310 3c,d) when the residence time of water was the longest (Figure 3d). The sharp decrease of
311 CH₄ storage and concentration in the transition from the WW to the CD seasons is
312 concomitant with a sharp increase of O₂ concentration at the bottom (up to $160 \pm 89 \mu\text{mol L}^{-1}$,
313 Figure 3).

314 During the three and a half years of monitoring, the same seasonal pattern as described above
315 is observed although the annual CH₄ bottom concentration and storage was threefold higher in
316 2009 and 2010 than in the year 2011 (Figure 3c,d). In the dry year 2012, the reservoir bottom
317 CH₄ concentration and storage was almost twice higher than in wet year 2011.

318 **3.3. Aerobic CH₄ oxidation in the reservoir**

319 Between 2010 and 2012, the depth integrated aerobic CH₄ oxidation rates ranged between
320 0.05 and 380 mmol m⁻² d⁻¹ at the stations RES1-RES8 (Figure 4). On average, aerobic
321 oxidation was higher in the WW season ($55 \pm 63 \text{ mmol m}^{-2} \text{ d}^{-1}$) than in the CD ($30 \pm 46 \text{ mmol}$
322 $\text{m}^{-2} \text{ d}^{-1}$) and WD ($36 \pm 32 \text{ mmol m}^{-2} \text{ d}^{-1}$) seasons and it was not statistically different for the
323 three years. In the WD season, aerobic CH₄ oxidation was on average twice higher in 2010
324 than for the two following years whereas in the CD season, the highest aerobic oxidation rate
325 was observed in 2012.

326 **3.4. Spatial and seasonal variability of surface CH₄ concentration and diffusive fluxes** 327 **at the reservoir surface (RES1-RES8)**

328 The surface concentrations at the stations RES1-8 ranged from 0.02 to 150 $\mu\text{mol L}^{-1}$ and were
329 $2.0 \pm 10.5 \mu\text{mol L}^{-1}$ (median = 0.9), $1.5 \pm 5.5 \mu\text{mol L}^{-1}$ (median = 0.4) and $3.4 \pm 14.7 \mu\text{mol L}^{-1}$
330 (median = 0.2) on average for the CD, WD and WW season, respectively. The surface

331 concentration followed a loglogistic distribution, which indicates the existence of extremely
332 high values. This is confirmed by the fact that the skewness of the time series of the log of the
333 CH₄ concentrations for all stations is positive (Figure S3), especially at the stations RES1,
334 RES3 and RES7 for which the skewness is >1. Over the course of the three and a half year of
335 survey, the surface concentrations were not statistically different between all stations and no
336 statistically significant seasonal variations were observed because of the occurrence of
337 sporadic events at all season (Figure S2a). The normalized distribution of concentrations (in
338 log) according to seasons (Figure 5) indicates that these high concentrations were observed
339 without any clear seasonal trend at the station RES1, RES5 and RES6 (<1 up to 150 μmol L⁻¹).
340 At the stations RES2 and RES3, the concentrations up to 128 μmol L⁻¹ were mostly
341 observed in the CD season when the reservoir overturns. At the station RES4 located at the
342 Nam Xot and Nam Theun confluence and at the stations RES7 and RES8 both located in the
343 inflow region of the Nam Theun River, the high surface concentrations (up to 64.60 μmol L⁻¹)
344 were mostly observed during the WW season when the reservoir undergoes sporadic
345 destratification. The auto-correlation function of the time series of the log of the surface CH₄
346 concentrations and diffusive fluxes at the stations RES1-8 indicated that at all stations (except
347 RES1) have a memory effect of 30 to 40 days (Figure S1). This implies that with a sampling
348 frequency of 15 days, we captured most of the changes in the surface CH₄ concentrations. At
349 the station RES1, the changes in CH₄ concentrations are faster than at other stations and
350 would have deserved a monitoring with a frequency higher than 15 days.

351 During the monitoring at RES1-RES8 stations, the average diffusive flux was 2.8 ± 12.2
352 $\text{mmol m}^{-2} \text{d}^{-1}$ ranging from 0.01 to 201.86 $\text{mmol m}^{-2} \text{d}^{-1}$ without any clear interannual and
353 seasonal trends (Figure S2b). As for the concentrations, flux data followed a loglogistic
354 distribution. The median flux in the WD season is 40 to 80% higher than the median in the
355 WW and CD season, respectively. However, the average fluxes in the WW and CD season are
356 30% higher than in the WD season (Table 2). This confirms the presence of extremely high
357 values during WD and CD seasons, as expected from the surface concentrations. All seasons
358 together, around 7% of the diffusive fluxes that we observed were higher than 5 $\text{mmol m}^{-2} \text{d}^{-1}$
359 which corresponds to extremely high diffusive fluxes in comparison with data from the
360 literature for reservoirs and lakes (Bastviken et al., 2008;Barros et al., 2011). The median and
361 average of these extreme fluxes higher than 5 $\text{mmol m}^{-2} \text{d}^{-1}$ were 2 times higher in the WW
362 and CD seasons than in the WD season (Table 2).

363 At NT2, diffusive CH₄ fluxes covered the whole range of fluxes reported for tropical
364 reservoirs, depending on the season. Most of the fluxes at the NT2R Reservoir were around
365 one order of magnitude lower than the ones at Petit Saut Reservoir (French Guiana) just after
366 the impoundment (Galy-Lacaux et al., 1997), and in the same order of magnitude as reported
367 for reservoirs older by 10 to 18 years (Abril et al., 2005;Guerin et al., 2006;Kemenes et al.,
368 2007;Chanudet et al., 2011). However, some diffusive fluxes at the stations RES1-8 in the
369 WW and the CD seasons (up to 202 mmol m⁻² d⁻¹) are among the highest ever reported at the
370 surface of a hydroelectric reservoir or a lake (Bastviken et al., 2011;Barros et al., 2011) and
371 rivers downstream of dams (Abril et al., 2005;Guerin et al., 2006;Deshmukh et al., 2016).

372 **3.5. Surface methane concentrations and diffusive fluxes at the water intake (RES9)**

373 After the commissioning of the reservoir (Julian day 450), the concentrations at the stations
374 RES9 (Figure 6a) located at the water intake were up to 30 times higher than at any other
375 stations that is 36.6±35.8 μmol L⁻¹ (median = 24.3), 37.6±67.0 μmol L⁻¹ (median = 0.9) and
376 1.0±1.7 μmol L⁻¹ (median = 0.3) in the WD, WW and CD season, respectively. The surface
377 concentrations at RES9 were significantly higher in the WD and WW seasons than in the WW
378 and CD seasons (p = 0.0002 and Figure 6a). The highest concentration was observed each
379 year at the end of the WD season-beginning of the WW season in between June and August.
380 These maxima decreased from 215 μmol L⁻¹ in August 2010 to 87 μmol L⁻¹ in June 2012.

381 The diffusive fluxes ranged between 0.03 and 605.38 mmol m⁻² d⁻¹ (Figure 6b and Table 2).
382 On average, the CH₄ diffusive fluxes at RES9 were two to forty times higher than at the other
383 stations in the CD, WD and WW season. Diffusive fluxes at this station are usually higher
384 than 10 mmol m⁻² d⁻¹ from April to July that corresponds to the WD season and the very
385 beginning of the WW season. In 2010, diffusive fluxes were on average 241 ± 219 and 239 ±
386 228 mmol m⁻² d⁻¹ respectively for the WD and WW seasons. In 2011 and 2012, the fluxes
387 dropped down by a factor of two in the WD season (112 ± 110 mmol m⁻² d⁻¹) and almost by a
388 factor of forty in the WW season (6.8 ± 14.4 mmol m⁻² d⁻¹). Overall, emissions at RES9
389 decreased by a factor of two between 2010 and 2012.

390 At the water intake, CH₄ diffusive fluxes during the transition between the WD and WW
391 seasons (up to 600 mmol m⁻² d⁻¹) are the highest reported at the surface of an aquatic
392 ecosystem (Abril et al., 2005;Guerin et al., 2006;Bastviken et al., 2011;Barros et al.,
393 2011;Deshmukh et al., 2016).

394 4. Discussion

395 4.1. CH₄ dynamic in the reservoir water column

396 The gradual decrease of the CH₄ concentration from the anoxic bottom water column to the
397 metalimnion and the sharp decrease around the oxicleine in the metalimnion (Figure 2) is
398 typical in reservoirs and lakes where CH₄ is produced in anoxic sediments and flooded soils
399 (Guerin et al., 2008;Sobek et al., 2012;Maeck et al., 2013), and where most of it is oxidized at
400 the oxic-anoxic interface (Bedard and Knowles, 1997;Bastviken et al., 2002;Guerin and Abril,
401 2007;Deshmukh et al., 2016).

402 CH₄ concentrations and storage increase concomitantly with the surface water temperature
403 and the establishment of the thermal stratification during the WD season and peak at the end
404 of the WD season-beginning of the WW season (Figure 2 and 3). During the WW season,
405 CH₄ concentrations and storage decrease slowly (Figure 3) while aerobic methane oxidation
406 reaches its maximum (Figure 4). When the reservoir overturns at the beginning of the CD
407 season, the CH₄ hypolimnic concentrations and storage reach their minima (Figure 3). The
408 overturn favours the penetration of oxygen down to the bottom (Figure 2 and 3b). The sharp
409 decrease of the CH₄ concentrations and CH₄ storage during this period is expected to result
410 from sudden outgassing (Section 4.2) together with an enhancement of the aerobic CH₄
411 oxidation as already observed in lakes that overturn (Utsumi et al., 1998b;Utsumi et al.,
412 1998a;Kankaala et al., 2007;López Bellido et al., 2009;Schubert et al., 2010;Schubert et al.,
413 2012;Fernández et al., 2014). A large increase of the aerobic methane oxidation was only
414 observed in the CD season in the dry year 2012 (Figure 4) because the amount of hypolimnic
415 CH₄ to be oxidized at the beginning of the CD season was still high in the water column
416 (Figure 3c,d).

417 As the reservoir overturns during the period over which the water residence time is the longest
418 in the reservoir, the temporal evolution of the concentrations is anti-correlated with the
419 residence time (Figure 3c,d). The seasonal dynamics of the CH₄ in the monomictic NT2R
420 differs from permanently stratified reservoirs like Petit Saut Reservoir where CH₄
421 concentration increased with retention time (Abril et al., 2005). However, at the annual scale
422 the water residence time has a strong influence on CH₄ concentration and storage in the
423 reservoir. Before the reservoir was commissioned (April 2010), the water residence time was
424 up to 4 years and the CH₄ storage was up to four times higher than in 2011 and 2012 (Figure

425 3d). Although a decrease of concentration and storage with the age of the reservoir was
426 expected (Abril et al., 2005), the storage in the dry year 2012 was twice higher than in the wet
427 year 2011 due to an increase of the water residence time by 25% between 2011 and 2012. In
428 wet years like 2011, the thermal stratification is weaker than in dry years since the warming of
429 surface water is less efficient and the high water inputs alters the stability of the reservoir
430 thermal stratification as shown by the sharper decrease and the larger range of ΔT in 2011
431 than in 2012 (Figure 3a). As a consequence, the oxygen diffusion to the hypolimnion was
432 higher in 2011 than in 2012 (Figure 3b) and it enhanced aerobic methane oxidation by 20% in
433 the water column in the WW season in 2011 as compared to 2012 (Figure 4). It therefore
434 suggests that the hydrology affects both the thermal stratification and the hypolimnic storage
435 of CH_4 in reservoirs, indirectly controls aerobic methane oxidation, and ultimately influences
436 emissions.

437 **4.2. Hot moments of emissions during sporadic destratification and reservoir overturn**

438 The figure 7 illustrates the evolution of the diffusive fluxes, the stratification index (ΔT), the
439 CH_4 storage and the aerobic CH_4 oxidation at the stations RES1, RES3, RES7 and RES8.
440 These four stations were selected for their contrasting skewness (Figure S3) which gives an
441 indication on the occurrence of extreme events and the facts that they are representative for all
442 station characteristics (Table 1). It shows that the large bursts of CH_4 (from 5 up to 200 mmol
443 $\text{m}^{-2} \text{d}^{-1}$) always occurred when ΔT decreased sharply ($>4^\circ\text{C}$, Figure 7a,d,g,j) and are usually
444 followed by a sharp decrease of the CH_4 storage in the water column (Figure 7b,e,h,k). These
445 hot moments of emissions occurred mostly in the CD at the stations RES1 and RES3 whereas
446 it was in the WW season at the stations RES7 and RES8 (Figure 7). In the WD season,
447 diffusive fluxes gradually increased together with the CH_4 storage in the water column
448 (Figure 7a,d,g,j) and they remained always lower than 20 $\text{mmol m}^{-2} \text{d}^{-1}$. These sporadic high
449 fluxes occurred in the WD season at RES3, RES7 and RES8 (Figure 7d,g,j). They are usually
450 associated with ΔT variations lower than 2°C and the CH_4 storage decrease that is associated
451 with these fluxes is not as sharp as the one observed in the CD and WW season (Figure
452 7e,h,k).

453 We therefore confirm the occurrence of hot moments of emissions during the reservoir
454 overturn in the CD season as already observed in lakes that overturn in temperate regions
455 (Kankaala et al., 2007;López Bellido et al., 2009;Schubert et al., 2010;Schubert et al.,
456 2012;Fernández et al., 2014). The highest emissions determined at NT2R are one order of

457 magnitude higher than previously reported outgassing during overturn and they occur mostly
458 in the section of the reservoir that has the longest water residence time (RES1-3, Table 1) and
459 the largest CH₄ storage (Figure 7b,e,h,k). This suggests that the impact of reservoir overturn
460 can be very critical for the whole-reservoir CH₄ budget in tropical hydroelectric reservoirs and
461 especially in young ones where hypolimnic concentration could reach up to 1000 μmol L⁻¹.
462 Hot moments of emissions also occur during sporadic destratifications in the WW season in
463 the inflow region (RES4 and RES6-8) where the inflow of cool water from the watershed
464 might disrupt the thermal stratification in reservoirs. This is contrasting with the observations
465 in older reservoir than NT2R where high emissions from the inflow region were recently
466 attributed to an enhancement of CH₄ production fuelled by the sedimentation of organic
467 matter from the watershed (Musenze et al., 2014). The high emissions in the WD seasons
468 were associated with early rains and associated high winds that occur sometimes in the last
469 fifteen days of May. This shows that a moderate erosion of the stratification when hypolimnic
470 CH₄ concentrations are high could enhance vertical transport of CH₄ toward the surface and
471 emissions to the atmosphere. Basically, this intense monitoring shows that spatial and
472 temporal variations of CH₄ emissions are largely controlled by the hydrodynamics of the
473 reservoir with extreme emissions occurring mostly in the inflow region during the wet season
474 and mostly in area remotely located from the inflow zone and the riverbed during reservoir
475 overturns in the CD season. Even if less frequent, moderate erosion of the stable and steep
476 thermal stratification during warm seasons, could also lead to high emissions.

477 The evolution of depth-integrated aerobic CH₄ oxidation is not clearly related with the
478 reservoir overturns and the CH₄ burst (Figure 7). Significant increases in the aerobic CH₄
479 oxidation occurred mostly during the first half of the WD season when the stratification was
480 unstable and at the very beginning of the destratification in the WW, when ΔT started to
481 decrease. The oxidation could reach high values (up to 380 mmol m⁻² d⁻¹) during these two
482 periods since the yield of CH₄ in the water column to sustain the activity of methanotrophs is
483 higher than in the CD season when the reservoir overturns. It shows that in reservoirs or lakes
484 like NT2R that destratify progressively before the overturn, there is no substantial increase of
485 the CH₄ oxidation when the water body overturns as it could be observed in lakes that
486 overturn within a few days (Kankaala et al., 2007). In addition, the contribution of CH₄
487 oxidation to the total loss of CH₄ (sum of diffusion and oxidation) in the WD and WW
488 seasons was 90-95% during the entire monitoring whereas it was 85% in the CD season.
489 During overturns, a significant amount of CH₄ is oxidized (Utsumi et al., 1998a; Utsumi et al.,

490 1998b;Kankaala et al., 2007;Schubert et al., 2012) but it also indicates that the removal of
491 CH₄ during overturn is not as efficient as during seasons with a well established thermal
492 stratification.

493 During the periods with major loss in the CH₄ storage with concomitant CH₄ burst, we
494 compared the change in the yield of CH₄ with the sum of emissions and oxidation. Most of
495 the time, the emissions alone and/or the sum of emissions and oxidation were significantly
496 higher than the amount of CH₄ that was lost from the water column. At the Pääjärvi Lake in
497 Finland (López Bellido et al., 2009), the fact that measured or calculated emissions exceed the
498 loss of CH₄ in the water column was attributed to a probable underestimation of the CH₄
499 storage in the lake by under-sampling the shallow area of the lake. In this study, emissions,
500 storage and oxidation were estimated at the same stations, avoiding such sampling artefacts.
501 Therefore, it suggests that CH₄ is provided by lateral transport or by production in the flooded
502 soil and biomass (Guerin et al., 2008) at a higher rate than the total loss of CH₄ from the water
503 column by emissions and oxidation. This hypothesis could only be verified by a full CH₄
504 mass balance including production and total emissions from the reservoir, which is beyond
505 the scope of this article.

506 **4.3. Hot spot of emissions at the water intake (RES9)**

507 After the commissioning of the reservoir, the temperature and the oxygen and CH₄
508 concentrations were constant from the surface to the bottom of the reservoir at the vicinity of
509 the water intake. On the basis of physical modelling and measurements of water current
510 velocities (Chanudet et al., 2012), the vertical mixing at this station was attributed to the water
511 withdrawal at the intake generating turbulence and water currents over a surface area of 3
512 km². At this station, CH₄-rich water from the reservoir hypolimnion reached the surface and
513 led to diffusive fluxes up to 600 mmol m⁻² d⁻¹ in the WD-WW seasons (Figure 6b) whereas
514 fluxes are 3 orders of magnitude lower in the CD season. To the best of our knowledge, this is
515 the first time that a hotspot of emissions is reported upstream of a dam or an intake bringing
516 water to the turbines. At NT2, the intake is located at the bottom of a narrow and shallow
517 channel (depth =9-20 m) on the side of the reservoir. This design enhances horizontal water
518 current velocities, the vertical mixing and therefore the emissions. The existence of such a
519 hotspot at other reservoirs might be highly dependant on the design of the water intake (depth
520 among other parameters) and its effect on the hydrodynamics of the reservoir water column.

521 **4.4. Estimation of total diffusive fluxes from the reservoir**

522 Yearly emissions by diffusive fluxes peaked at more than 9 Gg(CH₄) in 2010 when the
523 reservoir was commissioned and they decreased down to ≈ 5 Gg(CH₄) in 2011 and 2012
524 (Figure 8a and Table 3). Yearly integrated at the whole reservoir surface, these emissions
525 correspond to diffusive fluxes of 1.5 to 4 mmol m⁻² d⁻¹. These emissions are significantly
526 lower than diffusive fluxes measured at the Petit Saut Reservoir during the first two years
527 after flooding but similar to those determined in the following years (Abril et al., 2005) and
528 values reported for diffusive fluxes from tropical reservoirs in Barros et al. (2011). In absence
529 of the extreme emissions (both hotspots and hot moments), diffusive emissions from NT2R
530 would have been one order of magnitude lower than emissions from tropical reservoirs as
531 expected from the lower flooded biomass compare to Amazonian reservoirs (Descloux et al.,
532 2011). Due to the specific dynamic of diffusive fluxes at NT2R, diffusion at the reservoir
533 surface contribute 18 to 27% of total emissions (Table 3) that is significantly higher than at
534 other reservoirs tropical reservoirs where it was measured (See Deshmukh et al., 2016 for a
535 detailed discussion).

536 Most of the increase of CH₄ emissions by diffusive fluxes from 4 to 9 Gg(CH₄) between 2009
537 and 2010 is due to very significant emissions of 2-3 Gg(CH₄) at the water intake (Figure 8a).
538 This outgassing of CH₄ was triggered by the vertical mixing generated by the withdrawal of
539 water from the reservoir to the turbines. Although the area under the influence of the water
540 intake is less than 1% of the total area of the reservoir, emissions at the water intake
541 contributed between 13 and 25% of total diffusive emissions and 4 to 10 % if considering
542 both ebullition and diffusion (Table 3). It is worth to note that emissions at this site are only
543 significant within 3-5 month per year at the end of the WD season-beginning of the WW
544 season when the storage of CH₄ reach its maximum in the reservoir (Figure 8b). This new
545 hotspot equals 20 to 40% of downstream emissions and contributes between 4 and 7% of total
546 emissions from the NT2 reservoir surface when including ebullition and downstream
547 emissions (Table 3 and (Deshmukh et al., 2016)). Very localized perturbation of the
548 hydrodynamics, especially in lakes or reservoirs with CH₄-rich hypolimnion, can generate
549 hotspots of emissions contributing significantly to the total emissions from a given ecosystem.
550 These hotspots could be found upstream of dams and water intake in reservoirs but also
551 around aeration stations based on air injection or artificial mixing that could be used for
552 improving water quality in water bodies (Wüest et al., 1992).

553 The contribution of extreme diffusive fluxes (> 5 up to $200 \text{ mmol m}^{-2} \text{ d}^{-1}$) to total emission by
554 diffusion range from 30 to 50% on a yearly basis (Figure 8a) and from 40 up to 70% on a
555 monthly basis (Figure 8b) although these hot moments represent less than 10% of the
556 observations during the monitoring. In the literature, the statistical distribution of CH_4
557 emissions dataset always follows heavy-tailed and right skewed distribution like the log-
558 normal, the Generalized Pareto Distribution (Windsor et al., 1992;Czepiel et al., 1993;Ramos
559 et al., 2006;DelSontro et al., 2011) or loglogistic (this study) which indicates that CH_4
560 emissions are always characterized by high episodic fluxes. The quantification of emissions
561 thus requires the highest spatial and temporal resolutions in order to capture as many hot
562 moments as possible. At a single station, extreme emission events never lasted more than 2
563 months (3 consecutive sampling dates) and probably lasted less than 15 days most of the time
564 (Figure 7). The auto-correlation function of the concentration time series indicate that a
565 minimum sampling frequency of 1 month is required in this monomictic reservoirs for an
566 accurate description of the change in the surface concentrations and estimation of the
567 emissions (Figure S1). A lower temporal resolution can significantly affect (positively or
568 negatively) the emissions factors of non-permanently stratified freshwater reservoirs. This is
569 particularly critical in the inflow regions when water inputs from the watershed increase in the
570 rainy season in all reservoirs and at the beginning of the overturn in regions of the world
571 where reservoirs are not permanently stratified like in Asia (Chanudet et al., 2011) which
572 concentrate 60% of the worldwide hydroelectric reservoirs (Kumar et al., 2011).

573 **5. Conclusion**

574 The fortnightly monitoring of CH_4 diffusive emissions at nine stations revealed complex
575 temporal and spatial variations that could hardly been characterized by seasonal sampling.
576 The highest emissions occur sporadically during hot moments in the rainy season and when
577 the reservoir overturns. In the rainy season, they mostly occur in the inflow region because the
578 increase of the discharge of cool water from the reservoir tributaries contributes to sporadic
579 thermal destratification. During the reservoir overturn, extreme emissions occur mostly in
580 area remotely located from the inflows and outflows that are supposed to have the highest
581 water residence time. It shows that diffusive emissions can be sporadically as high as
582 ebullition and that these hot moments could contribute very significantly to the total emissions
583 from natural aquatic ecosystems and reservoirs. Our results showing that a monthly frequency
584 monitoring is the minimum required to capture all emissions is probably not applicable to

585 every aquatic ecosystem. However, it suggests that quantification of emissions based on 2-4
586 campaigns in a year might significantly affect emissions factors and carbon budgets of
587 ecosystems under study.

588 We also identified a new hotspot of emissions upstream of the water intake resulting from the
589 artificial destratification of the water column due to horizontal and vertical mixing generated
590 by the water withdrawal. In the case of the NT2R, emissions from this site contribute up to
591 25% of total diffusive emissions over less than 1% of the total reservoir area. We highly
592 recommend measurements of diffusive fluxes around water intakes (immediately upstream of
593 dams, typically) in order to evaluate if such results can be generalized.

594 **Acknowledgements**

595 The authors thank everyone who contributed to the NT2 monitoring programme, especially
596 the Nam Theun 2 Power Company (NTPC) and Electricité de France (EDF) for providing
597 financial, technical and logistic support. We are also grateful to the Aquatic Environment
598 Laboratory of the Nam Theun 2 Power Company whose Shareholders are EDF, Lao Holding
599 State Enterprise and Electricity Generating Public Company Limited of Thailand. CD
600 benefited from a PhD grant by EDF.

601

602 **References**

- 603 Abril, G., Guerin, F., Richard, S., Delmas, R., Galy-Lacaux, C., Gosse, P., Tremblay, A.,
604 Varfalvy, L., Dos Santos, M. A., and Matvienko, B.: Carbon dioxide and methane emissions
605 and the carbon budget of a 10-year old tropical reservoir (Petit Saut, French Guiana), *Global*
606 *Biogeochem. Cycles*, 19, 10.1029/2005gb002457, 2005.
- 607 Abril, G., Commarieu, M.-V., and Guerin, F.: Enhanced methane oxidation in an estuarine
608 turbidity maximum, *Limnol. Oceanogr.*, 52, 470-475, 2007.
- 609 Barros, N., Cole, J. J., Tranvik, L. J., Prairie, Y. T., Bastviken, D., Huszar, V. L. M., del
610 Giorgio, P., and Roland, F.: Carbon emission from hydroelectric reservoirs linked to reservoir
611 age and latitude, *Nature Geosci*, 4, 593-596, 2011.
- 612 Bastviken, D., Ejlertsson, J., and Tranvik, L.: Measurement of methane oxidation in lakes: A
613 comparison of methods, *Environ. Sci. Technol.*, 36, 3354-3361, 10.1021/es010311p, 2002.
- 614 Bastviken, D., Cole, J. J., Pace, M. L., and Van de Bogert, M. C.: Fates of methane from
615 different lake habitats: Connecting whole-lake budgets and CH₄ emissions, *J. Geophys. Res.-*
616 *Biogeosci.*, 113, G02024
617 10.1029/2007jg000608, 2008.
- 618 Bastviken, D., Tranvik, L. J., Downing, J. A., Crill, P. M., and Enrich-Prast, A.: Freshwater
619 Methane Emissions Offset the Continental Carbon Sink, *Science*, 331, 50,
620 10.1126/science.1196808, 2011.
- 621 Bedard, C., and Knowles, R.: Some properties of methane oxidation in a thermally stratified
622 lake, *Can. J. Fish. Aquat.Sci.*, 54, 1639-1645, 1997.
- 623 Borges, A. V., Delille, B., Schiettecatte, L. S., Gazeau, F., Abril, G., and Frankignoulle, M.:
624 Gas transfer velocities of CO₂ in three European estuaries (Randers Fjord, Scheldt, and
625 Thames), *Limnol. Oceanogr.*, 49, 1630-1641, 2004.
- 626 Chanudet, V., Descloux, S., Harby, A., Sundt, H., Hansen, B. H., Brakstad, O., Serca, D., and
627 Guerin, F.: Gross CO₂ and CH₄ emissions from the Nam Ngum and Nam Leuk sub-tropical
628 reservoirs in Lao PDR, *Sci. Total Environ.*, 409, 5382-5391, 10.1016/j.scitotenv.2011.09.018,
629 2011.
- 630 Chanudet, V., Fabre, V., and van der Kaaij, T.: Application of a three-dimensional
631 hydrodynamic model to the Nam Theun 2 Reservoir (Lao PDR), *J. Great Lakes Res.*, 38, 260-
632 269, <http://dx.doi.org/10.1016/j.jglr.2012.01.008>, 2012.
- 633 Chen, H., Wu, Y., Yuan, X., Gao, Y., Wu, N., and Zhu, D.: Methane emissions from newly
634 created marshes in the drawdown area of the Three Gorges Reservoir, *J. Geophys. Res.*, 114,
635 D18301, doi:10.1029/2009JD012410, 2009.
- 636 Chen, H., Yuan, X., Chen, Z., Wu, Y., Liu, X., Zhu, D., Wu, N., Zhu, Q. a., Peng, C., and Li,
637 W.: Methane emissions from the surface of the Three Gorges Reservoir, *J. Geophys. Res.*,
638 116, D21306, 10.1029/2011jd016244, 2011.
- 639 Czepiel, P. M., Crill, P. M., and Harriss, R. C.: Methane emissions from municipal
640 wastewater treatment processes, *Environ. Sci. Technol.*, 27, 2472-2477,
641 10.1021/es00048a025, 1993.
- 642 Delignette-Muller, M. L., Dutang, C., Pouillot, R., and Denis, J.-B.: An R Package for Fitting
643 Distributions, 1.0-4, 2015
- 644 DelSontro, T., McGinnis, D. F., Sobek, S., Ostrovsky, I., and Wehrli, B.: Extreme Methane
645 Emissions from a Swiss Hydropower Reservoir: Contribution from Bubbling Sediments,
646 *Environ. Sci. Technol.*, 44, 2419-2425, 10.1021/es9031369, 2010.
- 647 DelSontro, T., Kunz, M. J., Kempter, T., Wüest, A., Wehrli, B., and Senn, D. B.: Spatial
648 Heterogeneity of Methane Ebullition in a Large Tropical Reservoir, *Environ. Sci. Technol.*,
649 45, 9866-9873, 10.1021/es2005545, 2011.

650 Descloux, S., Chanudet, V., Poilvé, H., and Grégoire, A.: Co-assessment of biomass and soil
651 organic carbon stocks in a future reservoir area located in Southeast Asia, *Environ. Monit.*
652 *Assess.*, 173, 723-741, 10.1007/s10661-010-1418-3, 2011.

653 Descloux, S., Guedant, P., Phommachanh, D., and Luthi, R.: Main features of the Nam Theun
654 2 hydroelectric project (Lao PDR) and the associated environmental monitoring programmes,
655 *Hydroécol. Appl.*, 10.1051/hydro/2014005 2014, 2014.

656 Deshmukh, C., Serca, D., Delon, C., Tardif, R., Demarty, M., Jarnot, C., Meyerfeld, Y.,
657 Chanudet, V., Guedant, P., Rode, W., Descloux, S., and Guerin, F.: Physical controls on CH₄
658 emissions from a newly flooded subtropical freshwater hydroelectric reservoir: Nam Theun 2,
659 *Biogeosciences*, 11, 4251-4269, 10.5194/bg-11-4251-2014, 2014.

660 Deshmukh, C., Guérin, F., Labat, D., Pighini, S., Vongkhamsoo, A., Guédant, P., Rode, W.,
661 Godon, A., Chanudet, V., Descloux, S., and Serça, D.: Low methane (CH₄) emissions
662 downstream of a monomictic subtropical hydroelectric reservoir (Nam Theun 2, Lao PDR),
663 *Biogeosciences*, 13, 1919-1932, 10.5194/bg-13-1919-2016, 2016.

664 Dumestre, J. F., Guezennec, J., Galy-Lacaux, C., Delmas, R., Richard, S., and Labroue, L.:
665 Influence of Light Intensity on Methanotrophic Bacterial Activity in Petit Saut Reservoir,
666 French Guiana, *Appl. Environ. Microbiol.*, 65, 534-539, 1999.

667 Fernández, J. E., Peeters, F., and Hofmann, H.: Importance of the Autumn Overturn and
668 Anoxic Conditions in the Hypolimnion for the Annual Methane Emissions from a Temperate
669 Lake, *Environ. Sci. Technol.*, 48, 7297-7304, 10.1021/es4056164, 2014.

670 Galy-Lacaux, C., Delmas, R., Jambert, C., Dumestre, J. F., Labroue, L., Richard, S., and
671 Gosse, P.: Gaseous emissions and oxygen consumption in hydroelectric dams: A case study in
672 French Guyana, *Global Biogeochem. Cycles*, 11, 471-483, 1997.

673 Gross, J., and Ligges, U.: Tests for Normality (Nortest), 1.04-4, 2015

674 Guerin, F., Abril, G., Richard, S., Burban, B., Reynouard, C., Seyler, P., and Delmas, R.:
675 Methane and carbon dioxide emissions from tropical reservoirs: Significance of downstream
676 rivers, *Geophys. Res. Lett.*, 33, 10.1029/2006gl027929, 2006.

677 Guerin, F., and Abril, G.: Significance of pelagic aerobic methane oxidation in the methane
678 and carbon budget of a tropical reservoir, *J. Geophys. Res.-Biogeosci.*, 112,
679 10.1029/2006jg000393, 2007.

680 Guerin, F., Abril, G., Serca, D., Delon, C., Richard, S., Delmas, R., Tremblay, A., and
681 Varfalvy, L.: Gas transfer velocities of CO₂ and CH₄ in a tropical reservoir and its river
682 downstream, *J. Mar. Syst.*, 66, 161-172, 10.1016/j.jmarsys.2006.03.019, 2007.

683 Guerin, F., Abril, G., de Junet, A., and Bonnet, M.-P.: Anaerobic decomposition of tropical
684 soils and plant material: Implication for the CO₂ and CH₄ budget of the Petit Saut Reservoir,
685 *Appl. Geochem.*, 23, 2272-2283, 10.1016/j.apgeochem.2008.04.001, 2008.

686 Jahne, B., Munnich, K. O., Bosinger, R., Dutzi, A., Huber, W., and Libner, P.: On the
687 parameters influencing air-water gas-exchange, *J. Geophys. Res. Oceans*, 92, 1937-1949,
688 1987.

689 Kankaala, P., Taipale, S., Nykanen, H., and Jones, R. I.: Oxidation, efflux, and isotopic
690 fractionation of methane during autumnal turnover in a polyhumic, boreal lake, *J. Geophys.*
691 *Res.-Biogeosci.*, 112, G02003
692 10.1029/2006jg000336, 2007.

693 Kemenes, A., Forsberg, B. R., and Melack, J. M.: Methane release below a tropical
694 hydroelectric dam, *Geophys. Res. Lett.*, 34, L12809 10.1029/2007gl029479, 2007.

695 Kumar, A., Schei, T., Ahenkorah, A., Rodriguez, R. C., Devernay, J.-M., Freitas, M., Hall, D.,
696 Killington, A., and Liu, Z.: *Hydropower*, Cambridge, United Kingdom and New York, NY,
697 USA., 437-496, 2011.

698 López Bellido, J., Tulonen, T., Kankaala, P., and Ojala, A.: CO₂ and CH₄ fluxes during
699 spring and autumn mixing periods in a boreal lake (Pääjärvi, southern Finland), *J. Geophys.*
700 *Res.-Biogeosci.*, 114, G04007, 10.1029/2009JG000923, 2009.

701 MacIntyre, S., Jonsson, A., Jansson, M., Aberg, J., Turney, D. E., and Miller, S. D.: Buoyancy
702 flux, turbulence, and the gas transfer coefficient in a stratified lake, *Geophys. Res. Lett.*, 37,
703 L24604, 10.1029/2010GL044164, 2010.

704 Maeck, A., DelSontro, T., McGinnis, D. F., Fischer, H., Flury, S., Schmidt, M., Fietzek, P.,
705 and Lorke, A.: Sediment Trapping by Dams Creates Methane Emission Hot Spots, *Environ.*
706 *Sci. Technol.*, 47, 8130-8137, 10.1021/es4003907, 2013.

707 McClain, M. E., Boyer, E. W., Dent, C. L., Gergel, S. E., Grimm, N. B., Groffman, P. M.,
708 Hart, S. C., Harvey, J. W., Johnston, C. A., Mayorga, E., McDowell, W. H., and Pinay, G.:
709 Biogeochemical hot spots and hot moments at the interface of terrestrial and aquatic
710 ecosystems, *Ecosystems*, 6, 301-312, 10.1007/s10021-003-0161-9, 2003.

711 Musenze, R. S., Grinham, A., Werner, U., Gale, D., Sturm, K., Udy, J., and Yuan, Z.:
712 Assessing the Spatial and Temporal Variability of Diffusive Methane and Nitrous Oxide
713 Emissions from Subtropical Freshwater Reservoirs, *Environ. Sci. Technol.*, 48, 14499-14507,
714 10.1021/es505324h, 2014.

715 NTPC: Environmental Assessment and Management Plan - Nam Theun 2 Hydroelectric
716 Project. Nam Theun 2 Power Company, NTPC (Nam Theun 2 Power Company), Vientiane,
717 212, 2005.

718 Pacheco, F. S., Soares, M. C. S., Assireu, A. T., Curtarelli, M. P., Roland, F., Abril, G., Stech,
719 J. L., Alvalá, P. C., and Ometto, J. P.: The effects of river inflow and retention time on the
720 spatial heterogeneity of chlorophyll and water-air CO₂ fluxes in a tropical hydropower
721 reservoir, *Biogeosciences*, 12, 147-162, 10.5194/bg-12-147-2015, 2015.

722 R Development Core Team: R: A Language and Environment for Statistical Computing, R
723 Foundation for Statistical Computing, Vienna, Austria, 3-900051-07-0, 2008

724 Ramos, F. M., Lima, I. B. T., Rosa, R. R., Mazzi, E. A., Carvalho, J. o. C., Rasera, M. F. F.
725 L., Ometto, J. P. H. B., Assireu, A. T., and Stech, J. L.: Extreme event dynamics in methane
726 ebullition fluxes from tropical reservoirs, *Geophys. Res. Lett.*, 33, L21404,
727 10.1029/2006gl027943, 2006.

728 Schubert, C., Lucas, F., Durisch-Kaiser, E., Stierli, R., Diem, T., Scheidegger, O., Vazquez,
729 F., and Müller, B.: Oxidation and emission of methane in a monomictic lake (Rotsee,
730 Switzerland), *Aquat. Sci.*, 72, 455-466, 10.1007/s00027-010-0148-5, 2010.

731 Schubert, C. J., Diem, T., and Eugster, W.: Methane Emissions from a Small Wind Shielded
732 Lake Determined by Eddy Covariance, Flux Chambers, Anchored Funnels, and Boundary
733 Model Calculations: A Comparison, *Environ. Sci. Technol.*, 46, 4515-4522,
734 10.1021/es203465x, 2012.

735 Sobek, S., DelSontro, T., Wongfun, N., and Wehrli, B.: Extreme organic carbon burial fuels
736 intense methane bubbling in a temperate reservoir, *Geophys. Res. Lett.*, 39, L01401,
737 10.1029/2011gl050144, 2012.

738 St Louis, V. L., Kelly, C. A., Duchemin, E., Rudd, J. W. M., and Rosenberg, D. M.: Reservoir
739 surfaces as sources of greenhouse gases to the atmosphere: A global estimate, *Bioscience*, 50,
740 766-775, 2000.

741 Sturm, K., Yuan, Z., Gibbes, B., Werner, U., and Grinham, A.: Methane and nitrous oxide
742 sources and emissions in a subtropical freshwater reservoir, South East Queensland, Australia,
743 *Biogeosciences*, 11, 5245-5258, 10.5194/bg-11-5245-2014, 2014.

744 Teodoru, C. R., Bastien, J., Bonneville, M.-C., del Giorgio, P. A., Demarty, M., Garneau, M.,
745 Hélie, J.-F., Pelletier, L., Prairie, Y. T., Roulet, N. T., Strachan, I. B., and Tremblay, A.: The
746 net carbon footprint of a newly created boreal hydroelectric reservoir, *Global Biogeochem.*
747 *Cycles*, 26, GB2016, 10.1029/2011gb004187, 2012.

748 Utsumi, M., Nojiri, Y., Nakamura, T., Nozawa, T., Otsuki, A., and Seki, H.: Oxidation of
749 dissolved methane in a eutrophic, shallow lake: Lake Kasumigaura, Japan, *Limnol.*
750 *Oceanogr.*, 43, 471-480, 1998a.
751 Utsumi, M., Nojiri, Y., Nakamura, T., Nozawa, T., Otsuki, A., Takamura, N., Watanabe, M.,
752 and Seki, H.: Dynamics of dissolved methane and methane oxidation in dimictic Lake Nojiri
753 during winter, *Limnol. Oceanogr.*, 43, 10-17, 1998b.
754 Wanninkhof, R.: Relationship between wind-speed and gas-exchange over the ocean, *J.*
755 *Geophys. Res. Oceans*, 97, 7373-7382, 1992.
756 Windsor, J., Moore, T. R., and Roulet, N. T.: Episodic fluxes of methane from subarctic fens,
757 *Can. J. Soil Sci.*, 72, 441-452, doi:10.4141/cjss92-037, 1992.
758 Wüest, A., Brooks, N. H., and Imboden, D. M.: Bubble plume modeling for lake restoration,
759 *Water Resour. Res.*, 28, 3235-3250, 10.1029/92WR01681, 1992.
760 Yamamoto, S., Alcauskas, J. B., and Crozier, T. E.: Solubility of methane in distilled water
761 and seawater, *J. Chem. Eng. Data*, 21, 78-80, 10.1021/je60068a029, 1976.
762 Zheng, H., Zhao, X. J., Zhao, T. Q., Chen, F. L., Xu, W. H., Duan, X. N., Wang, X. K., and
763 Ouyang, Z. Y.: Spatial-temporal variations of methane emissions from the Ertan hydroelectric
764 reservoir in southwest China, *Hydrol. Processes*, 25, 1391-1396, 10.1002/hyp.7903, 2011.
765
766

767
768
769

Table 1: Characteristics of the nine monitoring stations in the Nam Theun 2 Reservoir

Station	Flooded ecosystem ¹	Hydrology	Water residence time index ²
RES1	Dense forest	100 m upstream of the Nakai Dam	**
RES2	Dense forest	Thalweg of the Nam Theun River	**
RES3	Dense forest	Embayment	***
RES4	Degraded forest	Confluence Nam Theun-Nam Xot Rivers	**
RES5	Degraded forest	Aside from the main stream	**
RES6	Degraded forest	Thalweg of the Nam Theun River	*
RES7	Swamp	Between inflows and water intake	*
RES8	Agricultural soils	Between inflows and water intake	*
RES9	Civil construction	Water intake	*

770 ¹Descloux et al. (2011)

771 ²Water renewal index in arbitrary units, (***) stands for longer residence time, (**) for
772 average residence times and (*) for shorter residence times than average for the whole
773 reservoir

774

775
776
777
778

Table 2 : Median, average, ranges and proportion of diffusive fluxes (F_{CH_4}) < 1 and > 5 mmol $m^{-1} d^{-1}$ for three seasons

Station		Warm Dry (WD)	Warm Wet (WW)	Cool Dry (CD)
RES1-RES8	n	212	252	217
	range	0.01-102.59	0.01-201.86	0.01-94.64
	median	1.08	0.64	0.20
	Average \pm SD	2.23 \pm 7.37	3.12 \pm 14.58	3.04 \pm 12.89
	% $F_{CH_4} < 1$	48%	63%	86%
	% $F_{CH_4} > 5$	6.6%	7.5%	7.4%
	Mediane $F > 5$	10.67	13.80	23.75
	Average $F > 5$	16.69 \pm 25.04	30.23 \pm 45.99	36.45 \pm 33.19
RES9	n	39	45	36
	range	0.24-342.00	0.03-605.38	0.07-17.62
	median	40.81	1.23	0.48
	average \pm SD	83.33 \pm 15.57	78.58 \pm 24.73	2.21 \pm 0.69

779
780

781 Table 3: Methane emissions from the Nam Theun 2 Reservoir between 2009 and 2012.

Gg(CH ₄) year ⁻¹	2009	2010	2011	2012
Emission from reservoir				
Diffusion at RES9 only	0.02±0.01	2.33±0.21	0.86±0.12	0.66±0.11
Total diffusion	4.45±1.01	9.34±2.32	3.71±0.81	4.95±1.09
Contribution of RES9 to diffusion (%)	0.4	24.9	23.2	13.3
Ebullition ¹	11.21±0.16	14.39±0.11	14.68±0.10	12.29±0.09
Total emissions from reservoir	15.66±1.02	23.73±2.32	18.39±0.82	17.25±1.09
Contribution of RES9 (%)	0.1	9.8	4.7	3.8
Total downstream emissions²	7.79±0.90	10.73±0.83	2.29±0.41	2.00±0.32
Total emissions (reservoir + downstream)	23.45±1.36	34.46±2.46	20.67±0.92	19.24±1.14
Contribution of diffusion to total emission	19%	27%	18%	26%
Contribution of RES9 to total (%)	<0.1	6.8	4.2	3.4

782 ¹Deshmukh et al. (2014)

783 ²(Deshmukh et al., 2016)

784

785

786
787 Figure captions

788
789 Figure 1: Map of the sampling stations and civil structures at the Nam Theun 2 Reservoir
790 (Lao PDR).

791
792 Figure 2: Vertical profiles of temperature ($^{\circ}\text{C}$), oxygen ($\mu\text{mol L}^{-1}$) and methane ($\mu\text{mol L}^{-1}$) at
793 the stations RES1, RES3, RES7, RES8 and RES9 in the Nam Theun 2 Reservoir.
794 Representative profile of the years 2010 (circle), 2011 (square) and 2012 (triangle) are given
795 for each seasons: cool dry in blue, warm dry in red, and warm wet in grey.

796
797 Figure 3: (a) Stratification index (ΔT , see text), (b) O_2 concentration in the hypolimnion
798 ($\mu\text{mol L}^{-1}$), (c) CH_4 concentration in the hypolimnion ($\mu\text{mol L}^{-1}$) and (d) CH_4 storage in the
799 water column ($\text{Gg}(\text{CH}_4) \text{ month}^{-1}$, bars) and water residence time (days, black line with circles)
800 in the Nam Theun 2 Reservoir (Lao PDR) between 2009 and 2012. The red, grey and blue
801 colours indicate the warm dry (WD), warm wet (WW) and cool dry (CD) seasons,
802 respectively. For the panels (a), (b) and (c), the boxes show the median and the interquartile
803 range, the whiskers denote the full range of values and the plus sign (+) denotes the mean.

804
805 Figure 4: Seasonal variations between 2010 and 2012 of the depth-integrated aerobic CH_4
806 oxidation ($\text{mmol m}^{-2} \text{ d}^{-1}$) at the stations RES1-RES8 calculated from the aerobic oxidation
807 rates determined by (Deshmukh et al., 2016). WD stands for warm dry (in red), WW for
808 warm wet (in grey) and CD for cool dry (in blue). The boxes show the median and the
809 interquartile range, the whiskers denote the full range of values and the plus sign (+) denotes
810 the mean.

811
812 Figure 5: Frequency distribution of the log of CH_4 concentrations ($\mu\text{mol L}^{-1}$) at the nine
813 monitoring stations of the Nam Theun 2 Reservoir. The red, grey and blue colours indicate the
814 warm dry (WD), warm wet (WW) and cool dry (CD) seasons, respectively.

815
816 Figure 6: (a) Surface concentrations and (b) diffusive fluxes between June 2009 and
817 December 2012 at the station RES9 located at the water intake. Julian day 0 is 1st of January,
818 2009. The red, grey and blue colours indicate the warm dry (WD), warm wet (WW) and cool
819 dry (CD) seasons, respectively.

820

821 Figure 7: (a, d, g, j) stratification index (ΔT , red line, see text) and diffusive fluxes, (b,e,h,k)
822 CH_4 storage and (c,f,i,l) depth-integrated aerobic CH_4 oxidation ($\text{mmol m}^{-2} \text{d}^{-1}$, black line)
823 calculated from the aerobic oxidation rates determined by (Deshmukh et al., 2016) and ΔT
824 (red line) between June 2009 and December 2012 at the stations RES1, RES3, RES7 and
825 RES8 at the Nam Theun 2 Reservoir. Julian day 0 is 1st of January, 2009. The red, grey and
826 blue colour dots indicate the warm dry (WD), warm wet (WW) and cold dry (CD) seasons,
827 respectively.

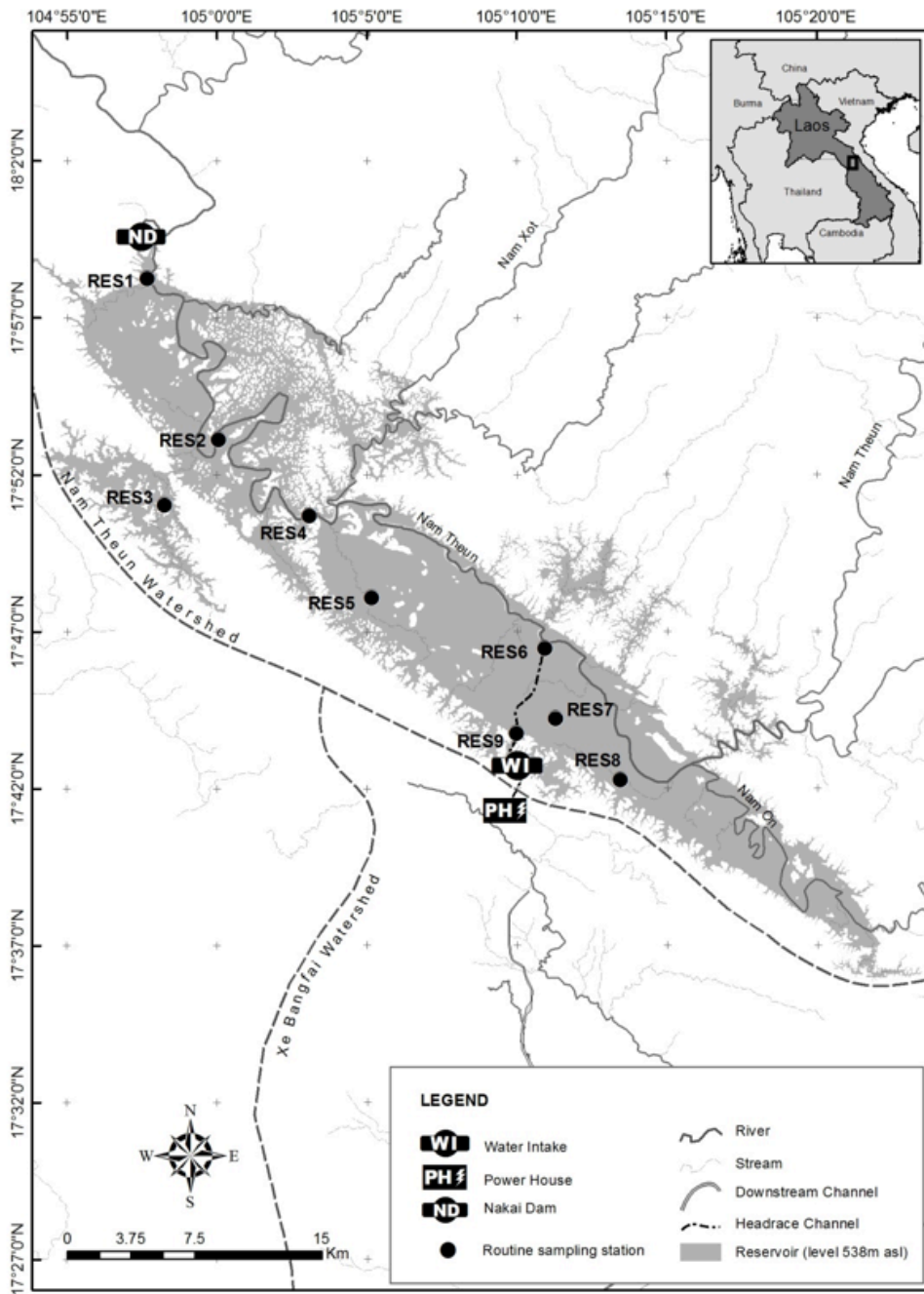
828

829 Figure 8: (a) Total emissions by diffusive fluxes in 2009, 2010, 2011 and 2012, and (b)
830 monthly emissions by diffusive fluxes between May 2009 and December 2012. Emissions
831 from RES9 (water intake) are shown in black, emissions resulting from diffusive fluxes lower
832 than $5 \text{ mmol m}^{-2} \text{d}^{-1}$ from the stations RES1 to RES8 are shown in white and emissions
833 resulting from diffusive fluxes higher than $5 \text{ mmol m}^{-2} \text{d}^{-1}$ from the stations RES1-RES8 are
834 shown in grey.

835

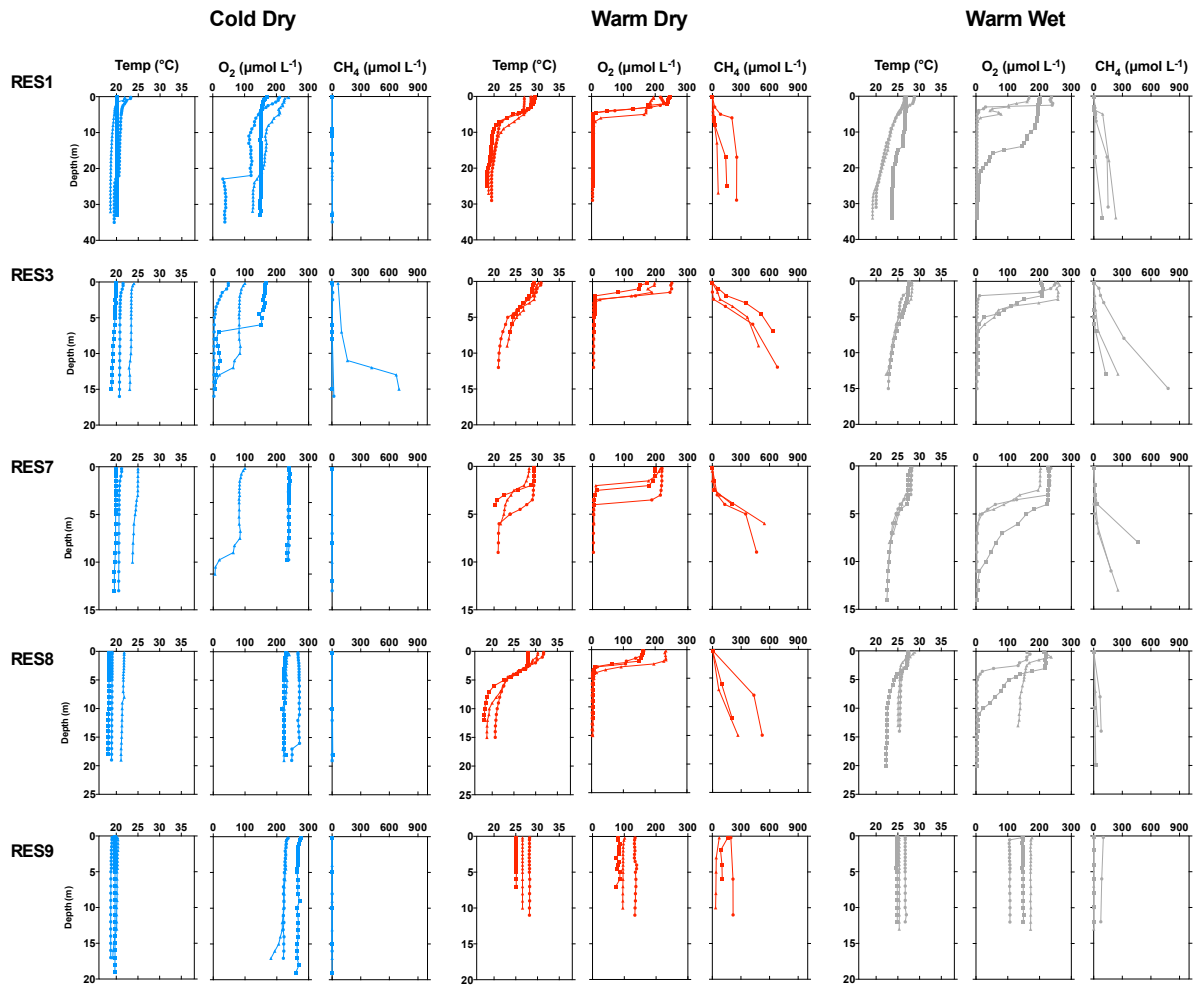
836

837
838 Figure 1
839



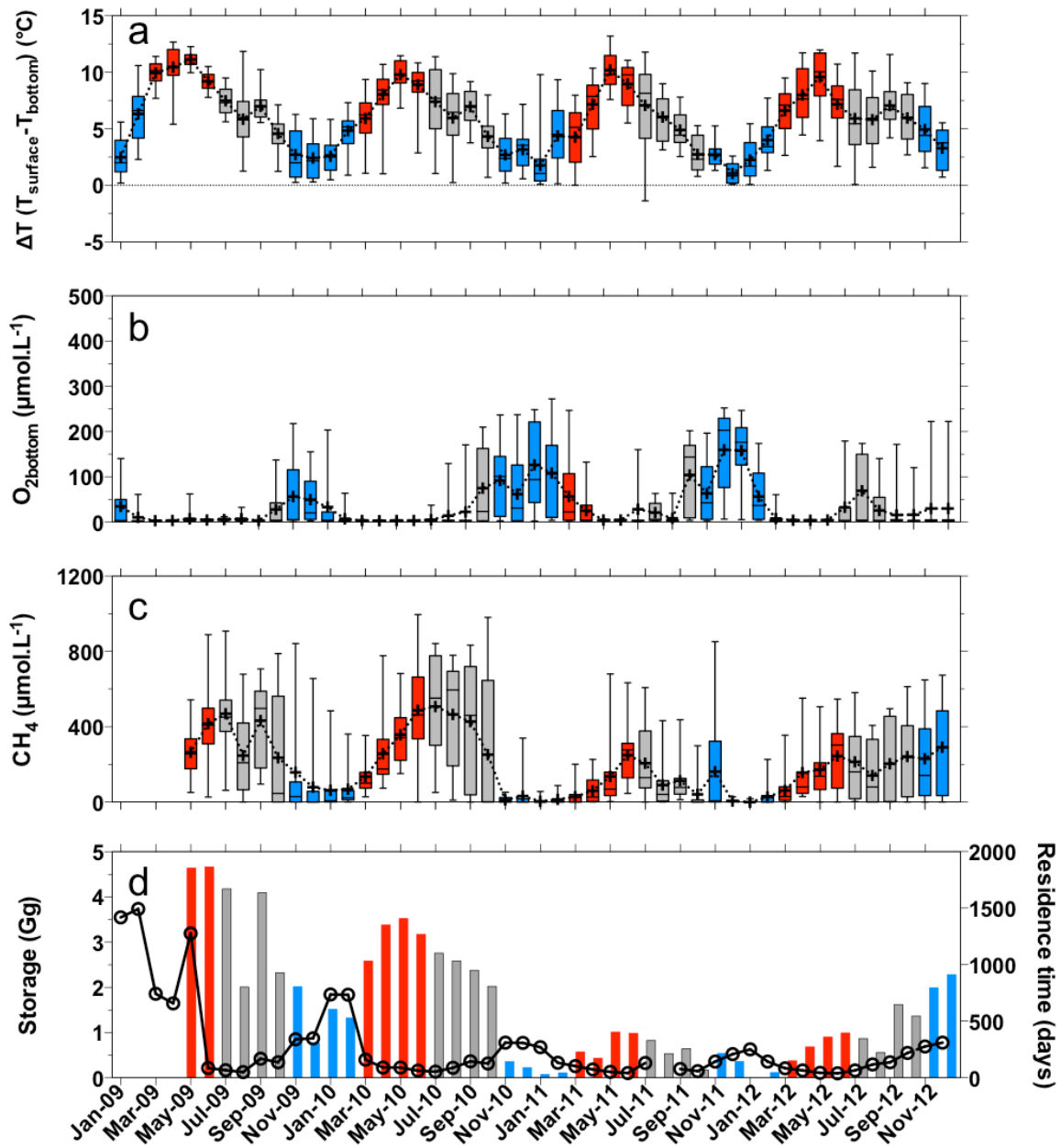
840
841
842

843
844 Figure 2
845



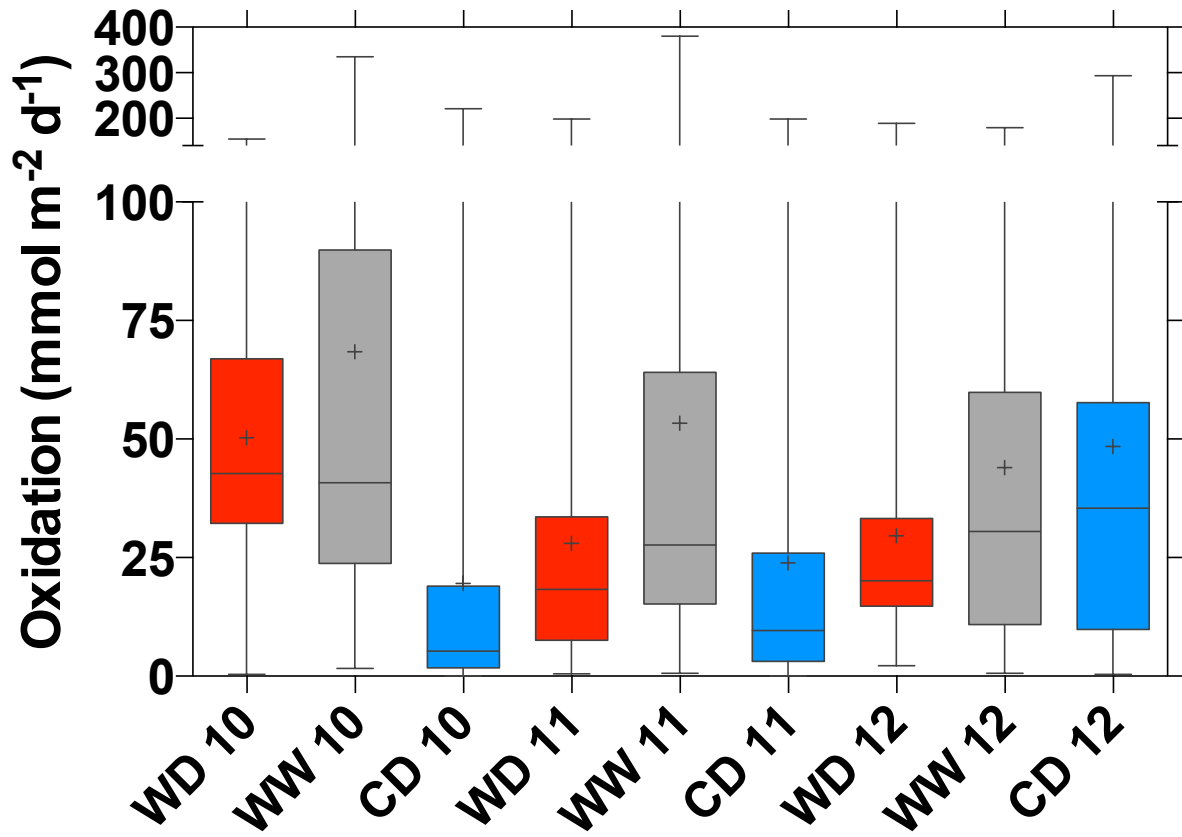
846
847
848

849
850 Figure 3
851



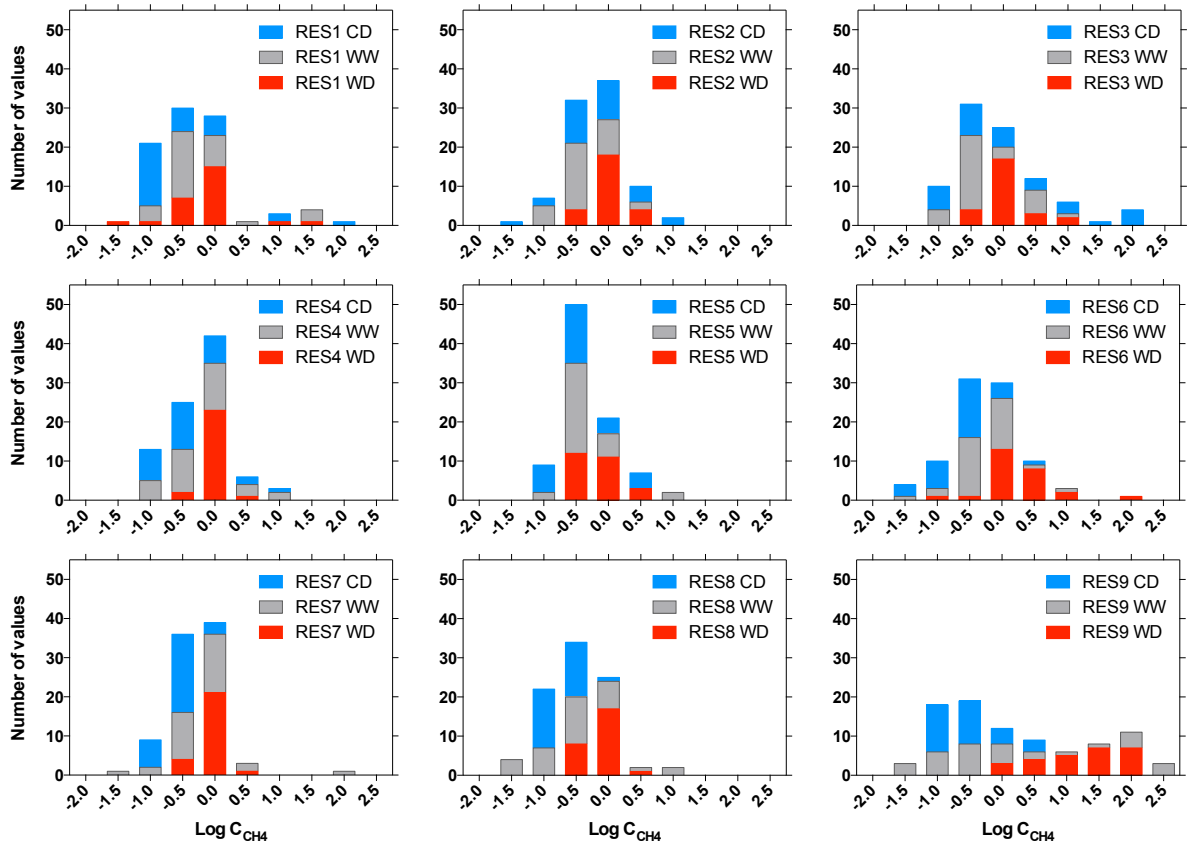
852
853
854

855
856 Figure 4
857



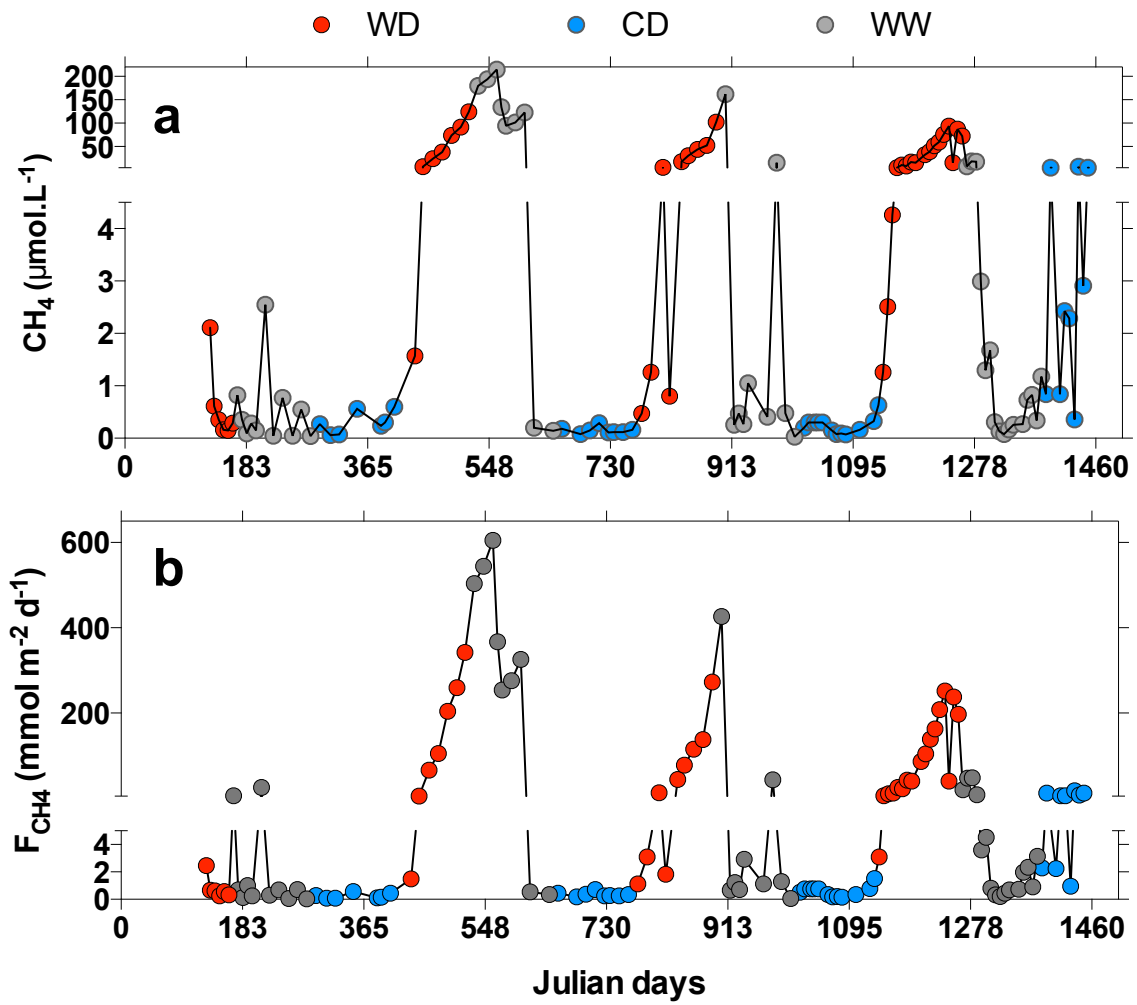
858
859
860

861
862 Figure 5
863



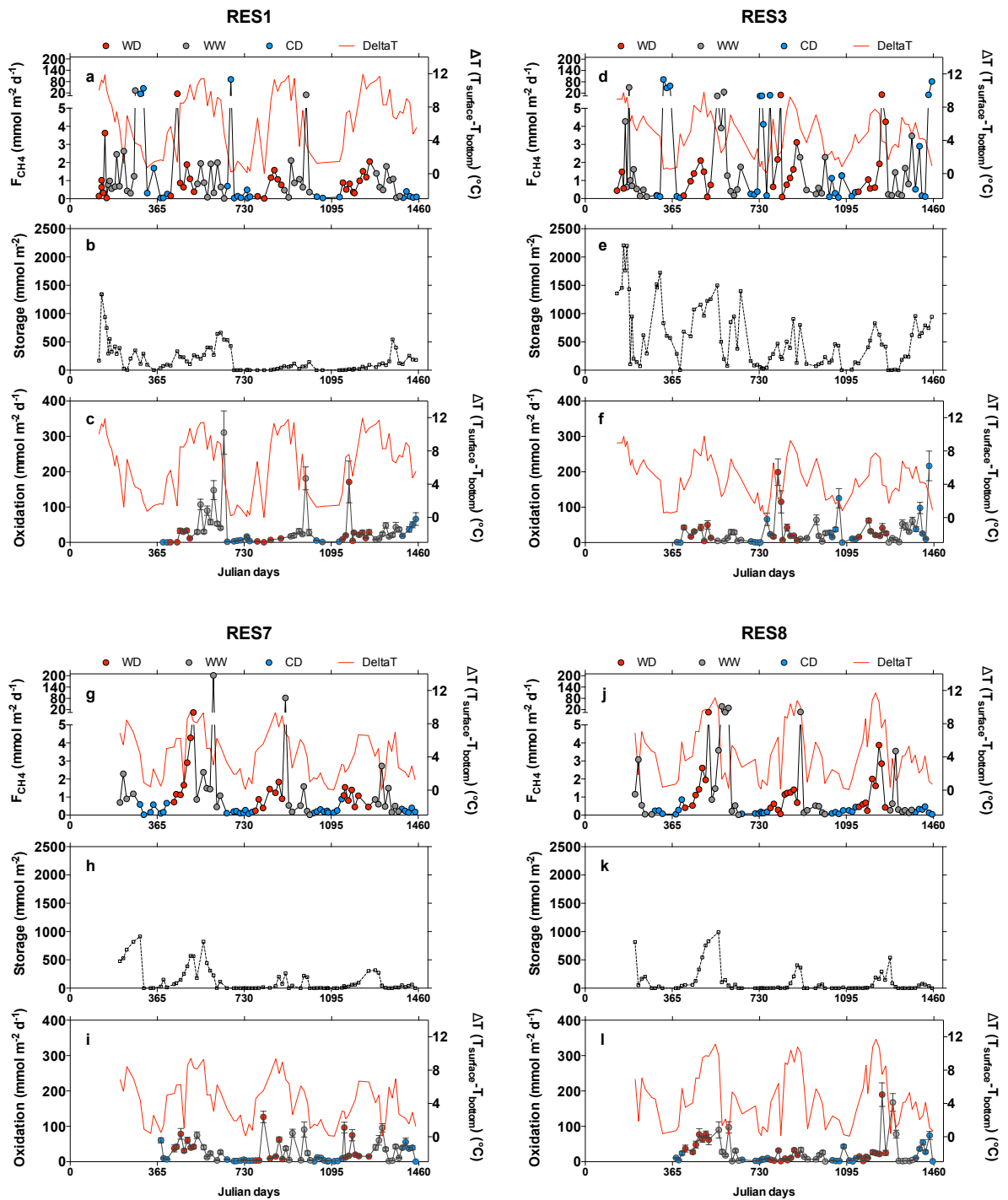
864
865
866

867
868 Figure 6
869



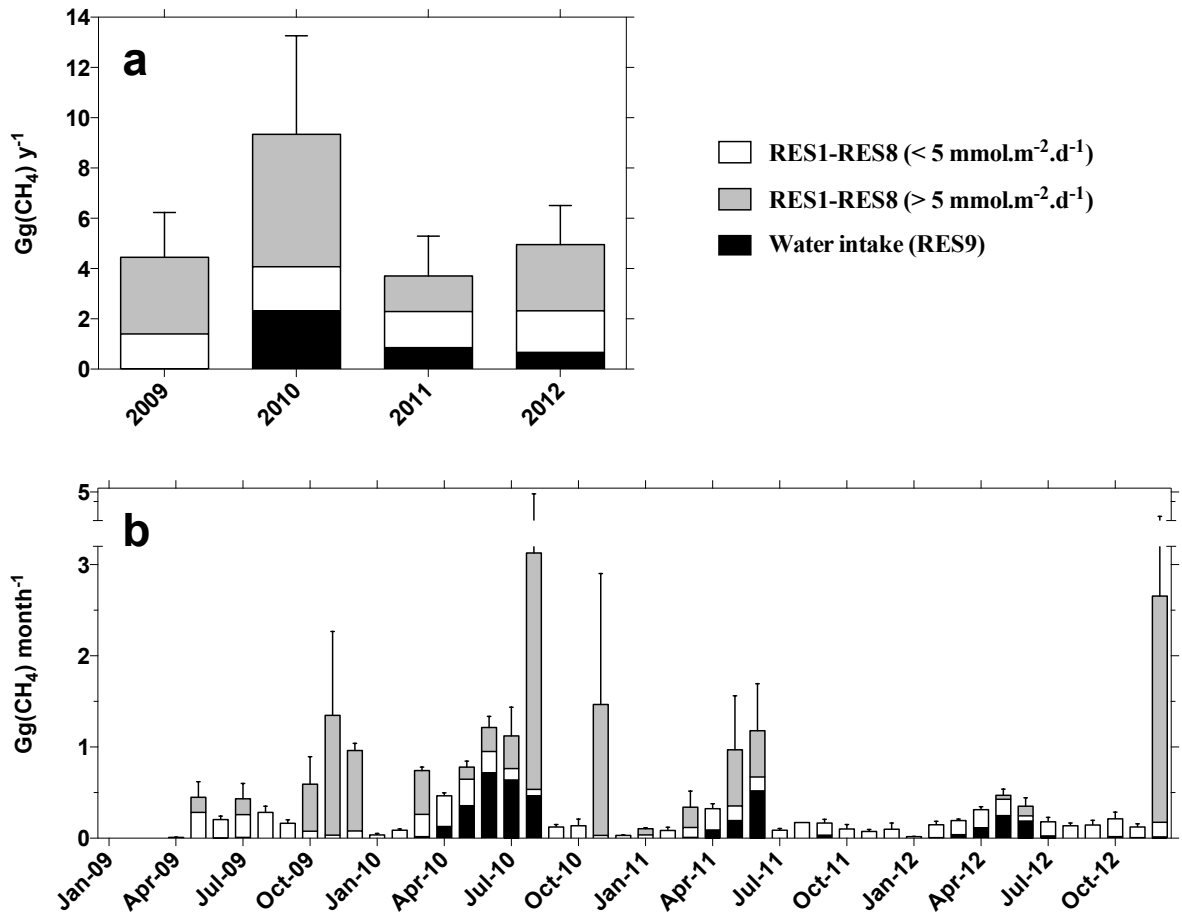
870
871
872

873
874 Figure 7
875



876
877
878

879
880 Figure 8
881



882